Improving directional adhesives with hierarchy

Aaron Parness,[1*] Noe Esparza,[1] Dan Soto[2] Others?[1] Mark Cutkosky[1]

[1]Department of Mechanical Engineering, Stanford University,
An Unknown Address, Stanford, CA 94305, USA
[2]Department of Applied Physics, Stanford University

[*]To whom correspondence should be addressed; E-mail: aaronparness@stanford.edu.

Many synthetic adhesives based on the gecko lizard have been fabricated, but as yet, these structures have not been employed in any real applications. Previous demonstrations have been limited to sample sizes of a few square centimeters, weights of a kilogram or less (often much less), and have only been performed on nanoscopically smooth surfaces like glass. By incorporating a hierarchical suspension into our dry adhesive, we have extended this performance several orders of magnitude to patch sizes greater than 100 cm^2, weights in excess of 35 kg, and have done so on both smooth and rough surfaces. The hierarchical adhesive was also applied to the Stickybot climbing robot platform, increasing maximum payload and range of climbable surfaces.

Hierarchical structures operate on multiple length scales providing compliance and an increased working range. Examples exist in nature in both plant and animal species providing super-hydrophopic or hydrophilic properties, high strength to weight ratios, and microscale dexterity within a large workspace (*1*).

The gecko's hierarchical adhesive system consists of mm scale lamellae, setae that are 30-

130 μm long and about 5 μm in diameter, setal branches that are 1 μm in diameter and a few μms long, and spatulae that are only 200 nm across and 10 nm thick (*2, 3*). While it is well documented that this compliant system allows geckos to stick to surfaces as smooth as glass and as rough as sandstone and tree bark using dry adhesion, little progress has been made incorporating hierarchy into synthetic dry adhesive structures. In fact, more than one hundred fabrication recipes have been developed for creating microstructures inspired by the gecko adhesive system (*4*) with only three groups demonstrating a hierarchical structure (*5–7*). The most notable single-layer adhesives include (*8–23*), and the performance of these structures and more are summarized conveniently in an online table (***?***). While (*5*)'s work explored the use of a two stage hierarchical adhesive, showing great improvement in the ability of their nanofeatures to conform and align to a spherical indenter, their structures were not reusable and showed minimal levels of adhesion making real world applications impractical. (*6*)'s hierarchical structures showed improved performance on rough surfaces because of the suspension structures ability to conform to changes in surface topography, but the hierarchical structures retained only 40$\%$ of the terminal features adhesive capability on glass due to a loss of real area of contact. (*7*)'s hierarchical structure also suffered from a loss of real contact area, showing a 10$\%$ improvement in performance. The film terminated suspension layer presented in this work does not limit the real area of contact while still providing the attractive advantages of a hierarchy: alignment forgiveness, conformation to rough surfaces, and equal load distribution, showing substantially improved performance on all surfaces.

Some modeling of hierarchical systems has also been completed predicting improved real area of contact with rough surfaces when compliance is increased through additional hierarchical levels or through the softening of suspension elements (*24–26*).

Previously, our group presented millimeter scale dry adhesive features consisting of angled polymer stalks with a sharp tip (*21*) which were used in the first successful climbing trials with

the Stickybot robot platform (*27*). More recently, a smaller 50 μm diameter wedge-shaped adhesive feature was presented showing improved performance in controlled laboratory tests on an experimental apparatus (*20*), but this adhesive design proved too sensitive to alignment and fabrication/surface irregularities to be useful on the climbing robot or in other real world applications. The first iteration of our hierarchical dry adhesive structure was fabricated by combining these two materials.

The two layers of the hierarchical structure were fabricated separately, and then bonded together using an inking process. In the first hierarchical design, the larger suspension stalks have a diameter of 380 μm and a vertical height of 1.0 mm. The stalk is angled 20 degrees off of vertical and has a beveled tip of 45 degrees which ends in a sharp point. These stalks are attached to a 1.0 mm thick backing layer. The structures are cast in a three part mold which was manufactured using a three axis CNC milling machine, described in detail in (*28*). The wedge shaped adhesive structures were cast from a mold created by a two step angled lithography procedure using SU-8, a photosensitive epoxy, described in detail in (*20*). They contact feature consists of a right-angle-wedge with a square base dimension of 50 μm and a vertical height of 200 μm. After the liquid polymer is cast under vaccuum, the mold is spun at constant RPM to control the uniformity of the backing layer to a few microns within a range of thickness from 100 μm to 400 μm. After patches of each of these materials were cut with a razor blade to the same approximate size, the tips of the larger suspension stalks were inked in a puddle of silicone based glue (Smooth On^{TM}Silpoxy)approximately 0.4 mm deep. The suspension structures were then placed face down onto the backing layer of the wedge shaped structures and allowed to bond. A picture of the completed hierarchy can be seen in 1.

The hierarchical structure's performance was tested against glass on an experimental apparatus consisting of three linear motion stages to control the sample's trajectory and a six axis force sensor to measure adhesive and shear forces, described more fully in (*20*). These data are

presented in 2 in the form of a limit surface (*29*), which shows combinations of forces for which the adhesive maintains contact, and the boundary at which the combination of shear and normal force causes contact failure by either detachment or sliding.

Three hierarchical designs were built in total, all showing a high directional dependence on adhesion consistent with the frictional adhesion model developed to describe gecko adhesion (*30*). Without shear loading, the samples displayed no adhesion, but when a shear load was applied in the preferred direction of the sample, the adhesives were activated, and substantial adhesive forces were demonstrated. Typical pressure-sensitive adhesives show the opposite behavior, having their strongest adhesive forces in purely normal loading scenarios and decreasing adhesive capability with increasing shear. The synthetic structures have *increasing* adhesion with increasing shear. The limit surfaces for frictional adhesives also cross the origin, indicating that when the shear load on the samples is released, they can detach from a surface with zero force. This is a very useful property for climbing applications where a patch must be attached and detached many times efficiently.

The hierarchical system also retained a property of the wedge-shaped adhesive previously termed 'dynamic adhesion' (*20*). When overloaded in pure shear, the sample fails in sliding while maintaining adhesive forces. This bulk behavior is caused by individual wedges detaching and reattaching as the sample slides. The property allows a sample to slide down a surface slowly rather than lose adhesion suddenly and fall catastrophically to the ground. Samples that exhibit dynamic adhesion are also able to arrest sliding when the overload pressure is released. Experimental measurements of the sliding adhesion can be seen in 2d and a demonstration of a hierarchical patch slipping via 'dynamic adhesion' is shown in supplementary video S1.

While the first hierarchical system retained the useful properties of the original wedge-shaped adhesive, the overall levels of sustainable adhesion decreased approximately 40 percent. This loss of adhesive pressure was due to uneven load distribution. Under load, the contacting

wedge layer buckled between adjacent suspension stalks causing a significant reduction in the number of wedges making good contact with a surface. In order to improve load sharing, the design of both the contacting features and the suspension structure were modified. Simple beam theory can be used as a very rough model of the deflections of the wedge backing layer between adjacent suspension stalks, and suggests that an increase in the thickness of the membrane or a decrease in the distance between suspension stalks would improve load sharing. These general guidelines were implemented in two successive hierarchical designs, and all three structures were later modeled using the Ansys finite element software package to more accurately understand load sharing and the contact mechanics of the suspension structures.

In the Hierarchy II design, new wedge-shaped structures that had a rectangular footprint of 20 μm by 200 μm and a height of 80 μm were more densely packed, improving the fill factor of the contact layer from 25% to 50%. The backing membrane of the wedge layer was also doubled in thickness to increase the resistance to deflections between adjacent hierarchical stalks discussed above. This change increased the maximum sustainable forces more than $2\times$. In the Hierarchy III design, the suspension structure was modified to further improve load sharing among contacts. Longer and more significantly angled posts were packed at a density of 2,000,000 per m^2, effectively halving the distance between adjacent suspension elements, L. These posts were angled at 35 degrees or 45 degrees off vertical and were fabricated from a stiffer polyurethane. These modifications improved adhesive performance by another $2\times$. Pictures of these structures and data from experimental trials on glass are shown in 2c.

In the finite element analysis, each hierarchy was modeled as a suspension layer consisting of pillar-like structures attached at the base, and a top membrane of material that represents the backing layer of the wedge features. The edges of the model are connected to form a periodic boundary condition which effectively models an infinite two-dimensional strip of the structure. During simulation, plane-stress was assumed with a finite thickness. The loading condition was

provided by a rigid plate pushing onto the structure along a 45 degree trajectory to a depth of 500 μms. Friction was assumed between the plate and hierarchical structure, and all models used the same friction parameters. The models differed in geometry and material parameters (measured empirically on an Instron tensile tester) to match the three hierarchy designs.

The max contact pressure decreases with each iteration of the hierarchy design as seen in Figure 3. Hierarchy I showed a max pressure of 62.8 kPa, Hierarchy II showed 43 kPa, and Hierarchy III only 23 kPa. The distribution of contact pressure became more uniform with each iteration of the hierarchy as well, indicating improved load sharing. Hierarchy I only generated approximately 10$\%$ intimate contact with the surface, while Hierarchy II and Hierarchy III showed 31$\%$ and 32$\%$ respectively. These numbers do not represent actual contact since the terminal wedge features were not modeled during this evaluation, and it is likely that the wedge features would further elongate the pressure distribution. One indication of this is that neither Hierarchy II nor Hierarchy III's terminal membrane displaced more than 10 μms from the contact surface. Further models are being developed as a predictive tool to continue improving the suspension structure's design.

The overall stiffness of each layer of the hierarchies was also analyzed to ensure compatibility. In order to be compatible, the suspension layer must be soft enough to correct for misalignments and surface irregularities, but stiff enough to force the wedge shaped features to bend and engage a significant potion of their angled face.

The stiffness of each layer was measured empirically. For the Hierarchy III design, measurements were made while each layer was compressed to 50$\%$ of its initial height. The stiffnesses were measured as 27,000 N/m per cm^2 for the wedge layer, 2000 N/m per cm^2 for the suspension layer, and 1500 N/m per cm^2 for the combined hierarchical system including the glue layer. Using the measured values for each layer and a theoretical preload of 10 kPa, the respective deflections within the structure can be calculated. The suspension posts should deflect 1.05 mm

(71% of their height) while the wedge structures would 36 μm (46% of their height). Video of the structure under an initial 10 kPa preload followed by a 1 mm horizontal drag is available as supplementary video S2.

Scaling

One of the primary limitations of single-layer fibrillar adhesive structures is their inability to be scaled to larger patch sizes. This is true of all gecko-like adhesives presented previously in the literature, none of which show data for patch sizes more than 4 cm^2. An experiment was performed on the wedge-shaped adhesive structures to show the effects of scaling. 8 patches that varied in size from 0.1 to 10 cm^2 were fabricated from the same mold and tested identically on the experimental apparatus. A significant drop off in both adhesive and shear pressure was observed for patches larger than about 1 cm^2. However, when the hierarchical adhesive was tested in the same type of experiment, no drop off was observed. These data are presented in 4a.

Single layer fibrillar arrays suffer from an extremely high demand on alignment for patch sizes above a few mm^2. Because the height of the features is so much smaller than the diameter of the sample, the patch must be presented in a flat-to-flat orientation to the surface with great angular precision. For example, if an 80 μm tall fiber like those used in the hierarchical system is mounted by itself on a rigid substrate, it may be tolerant to variation in the depth of load of about +- 20 μm at best. Across a 5 mm diameter patch, this would require an angular alignment of about 0.5 degrees, but for a patch of 10 cm diameter, an angular alignment of 0.02 degrees is required. This level of precision is difficult to attain on a well-controlled experimental platform, and becomes impossible to achieve in a real world application like a climbing robot. The hierarchical system, however, provides compliance that allows a 10 cm diameter patch to self-align to a surface and engage a high number of contacting fibers appropriately. The

hierarchical suspension layer can also compensate for irregularities in the contacting wedge layer that may have arisen during manufacture, or for abnormalities on a test surface.

It is important to note that a hierarchy cannot simply be compliant during loading, it must also distribute forces evenly to the many thousands of contacts. If an isotropic foam or soft rubber backing was used in place of the fibrillar suspension structures, this load sharing would not be accomplished. A stress concentration would exist at the leading or trailing edge of the patch (depending on load angle), and the patch would peel away from the surface at loads much less than those achieved with a fibrillar suspension structure. The angled nature of the suspension elements also matches the predominantly shear loading vector of a patch hanging on a vertical surface, which aids in load distribution.

To show the scalability of the hierarchical structure out to patch sizes of 100 cm^2 and greater, a second set of experiments were run where patches of various sizes were placed on a vertical glass surface and loaded with hanging weights. Square patches ranging from 6 cm^2 to 130 cm^2 were tested identically in this manner. Data from this experiment are presented in 4b. The largest patches still engaged greater than 80 percent of the contact layer, observed through the glass by a color change in the sample as seen in 4d. Patches larger than 25 cm^2 were fabricated by tiling together multiple pieces of both the suspension layer and the contacting layer, showing the Hierarchies' tolerance to manufacturing imprecision. These hang tests were repeated more than ten times each in order to demonstrate the reusability of the structures. The largest patch has been demonstrated more than 500 times without degradation of performance. If a patch becomes dirty, it can be cleaned with soap and water. Video of large patch demonstrations is available as supplementary movie S3.

Rough surfaces

The same basic principles of alignment tolerance, conformation to surface irregularities, and equal load distribution that permit the hierarchical structure to be scaled to large areas also enable its use on semi-rough surfaces like metal, plastic, and wood. These rougher surfaces are inherently unable to achieve flat-to-flat alignment since their surfaces are not actually flat. Therefore, for a patch of any size to adhere to a semi-rough surface, it must be able to locally self-align to the topography of that surface while still maintaining an even load distribution profile. The hierarchical suspension system presented here achieves these properties for surfaces with modest, slow-changing roughness. However, for sharp changes in roughness, the system is unable to accurately match the surface topography or is unable to pull with even pressure. This causes a loss of contact in certain areas. So, while film terminated suspension layers are effective for adhering to metals, plastic, wood, and interior walls, the maximum sustainable load drops off as roughness increases. Data for a variety of common surfaces are presented in 5 and a demonstration of the material's performance on common surfaces is shown in supplementary movie S3.

To conform to rougher surfaces like exterior walls, tree bark, and brick, future hierarchical designs will need to decouple the suspension layer and the contacting layer in such a way to allow larger scale conformation to sharp changes in roughness. With adjacent suspension elements linked by the backing membrane of the contact wedge layer, conformation to surfaces with sharp discontinuities of this type is not currently possible.

Applications and conclusion

The hierarchical dry adhesive was designed with robotic and human climbing applications in mind. The Stickybot robot platform (*27*) had previously only climbed with the mm-sized angled

polymer stalks (*21*), and hung statically from vertical glass with the 50 μm diameter wedge shaped adhesive (*20*). With the hierarchical system, the robot was able to climb vertical glass carrying a payload more than double its weight (robot weight is 400 g, payload was 1 kg), limited not by the adhesive capability, but by the strength of the compliant shoulder joint of the robot. The robot was also able to climb a new range of surfaces including wood panelling, metal cabinets, and other interior surfaces as seen in Figure 6. Video of these robotic demonstrations is available online as supplementary video S4.

Other real world applications should also now be possible with a hierarchical suspension layer like the one presented here. Hanging flatscreen televisions, mounting billboards to the sides of skyscrapers, and creating manufacturing fixtures are all fairly straightforward possibilities for this technology.

By incorporating a hierarchical suspension into our adhesive structure, we increased the usable patch size from 1 cm^2 to more than 100 cm^2, demonstrated reusable adhesion for weights in excess of 35 kg, and showed adhesion on semi-rough surfaces previously unresponsive to dry adhesives. The design of the hierarchical suspension structure should be universally applicable to all groups making gecko-like adhesives. Similar suspension structures would allow other fibrillar adhesives (some of which perform better than the wedge shaped adhesive presented with this work) to also be scaled to larger patch sizes and to perform on semi-rough surfaces.

References

1. B. Bhushan, *Philosophical Transactions of the Royal Society A* (2009).

2. K. Autumn (2006), pp. 225–256.

3. A. Russell, M. Johnson, S. Delannoy, *Journal of Adhesion Science and Technology* (2007).

4. A. del Campo, E. Arzt, *Chem. Rev* (2008).

5. M. Northen, K. Turner, *Sensors & Actuators: A. Physical* **130**, 583 (2006).

6. H. E. Jeong, J.-K. Lee, H. N. Kim, S. H. Moon, K. Y. Suh, *Proc Natl Acad Sci USA* **106**, 5639 (2009).

7. M. Murphy, S. Kim, M. Sitti, *ACS Applied Materials & Interfaces* **1**, 849 (2009).

8. L. Ge, S. Sethi, L. Ci, P. M. Ajayan, A. Dhinojwala, *Proc Natl Acad Sci USA* **104**, 10792 (2007).

9. S. Gorb, M. Varenberg, A. Peressadko, J. Tuma, *Journal of The Royal Society Interface* **4**, 271 (2006).

10. M. Murphy, B. Aksak, M. Sitti, *Small* (2008).

11. A. Mahdavi, L. Ferreira, C. Sundback, J. Nichol, *Proceedings of the National Academy of Sciences* (2008).

12. L. Qu, L. Dai, M. Stone, Z. Xia, Z. Wang, *Science* (2008).

13. M. T. Northen, C. Greiner, E. Arzt, K. L. Turner, *Adv. Mater.* **20**, 3905 (2008).

14. J. Lee, C. Majidi, B. Schubert, R. S. Fearing, *Journal of The Royal Society Interface* **5**, 835 (2008).

15. A. del Campo, C. Greiner, E. Arzt, *Langmuir* (2007).

16. H. Lee, B. P. Lee, P. B. Messersmith, *Nature* **448**, 338 (2007).

17. A. K. Geim, *et al.*, *Nat Mater* **2**, 461 (2003).

18. D. Kim, *et al.*, *Microsystem Technologies* (2007).

19. B. Schubert, J. Lee, C. Majidi, R. S. Fearing, *Journal of The Royal Society Interface* **5**, 845 (2008).

20. A. Parness, *et al.*, *Journal of the Royal Society, Interface* (2009).

21. D. Santos, M. Spenko, A. Parness, S. Kim, M. Cutkosky, *Journal of Adhesion Science and Technology* **21**, 1317 (2007).

22. Y. Zhao, T. Tong, L. Delzeit, A. Kashani, M. Meyyappan, *Journal of Vacuum Science & Technology B: Microelectronics* (2006).

23. E. Chan, E. Smith, R. Hayward, A. Crosby, *Adv. Mater.* **20**, 711 (2008).

24. B. Bhushan, *Journal of Adhesion Science and Technology* **21**, 1213 (2007).

25. B. Chen, P. Wu, H. Gao, *Proceedings of the Royal Society A: Mathematical, Physical and Engineering Sciences* **464**, 1639 (2008).

26. H. Yao, H. Gao, *Journal of Adhesion Science and Technology* (2007).

27. S. Kim, *et al.*, *Robotics, IEEE Transactions on [see also Robotics and Automation, IEEE Transactions on]* **24**, 65 (2008).

28. D. Santos, S. Kim, M. Spenko, A. Parness, M. Cutkosky, *IEEE ICRA* (2007).

29. S. Goyal, A. Ruina, J. Papadopoulos, *1989 IEEE International Conference on Robotics and Automation* (1989).

30. K. Autumn, A. Dittmore, D. Santos, M. Spenko, M. Cutkosky, *Journal of Experimental Biology* **209**, 3569 (2006).

Supporting Online Material www.sciencemag.org Movies S1, S2, S3, S4

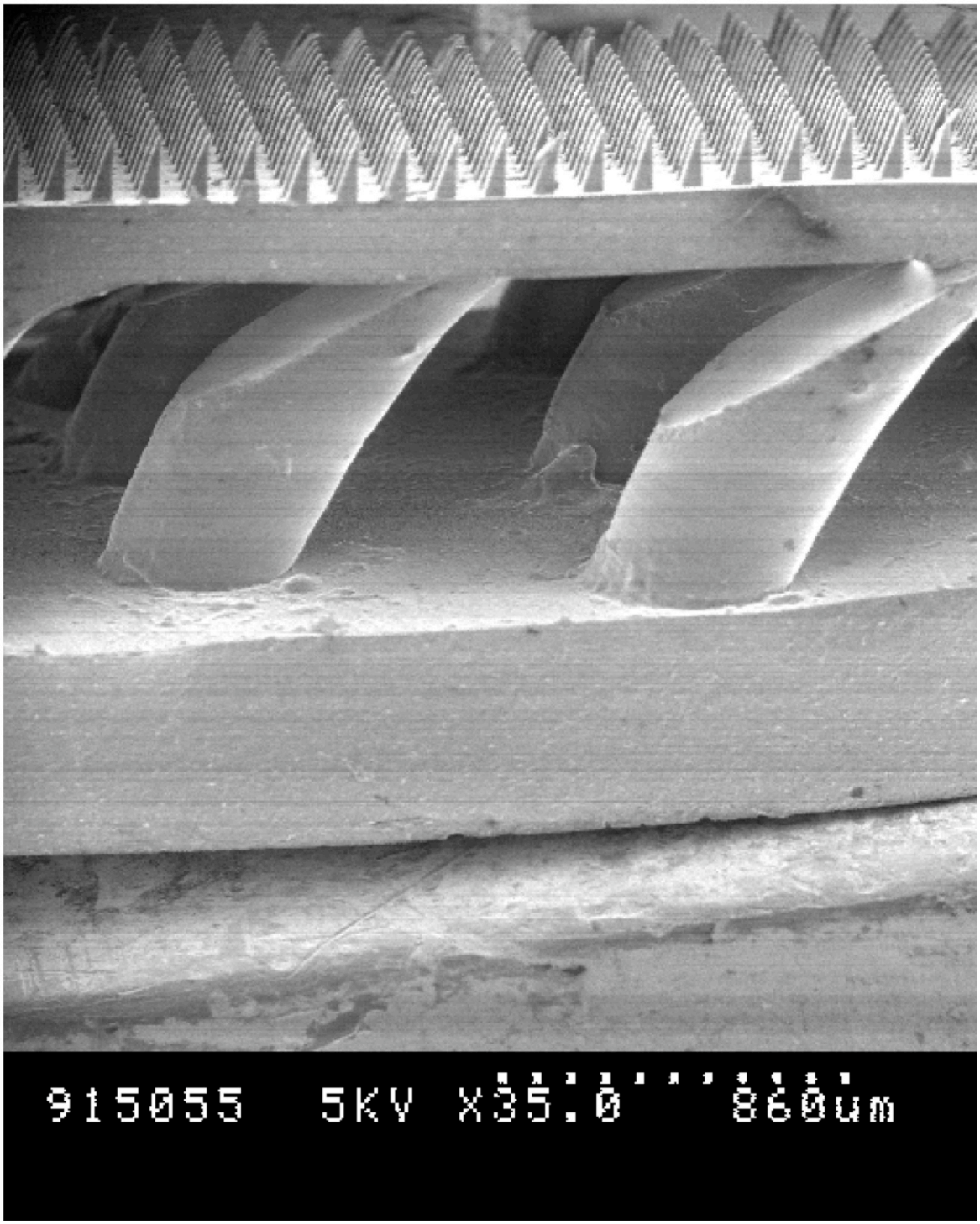

Figure 1: Hierarchy I consisting of a wedge-shaped adhesive layer mounted on a compliant suspension layer of tapered, angled posts. Both layers were cast separately out of silicone rubber and joined by an inking process with RTV 118 Silicone Adhesive.

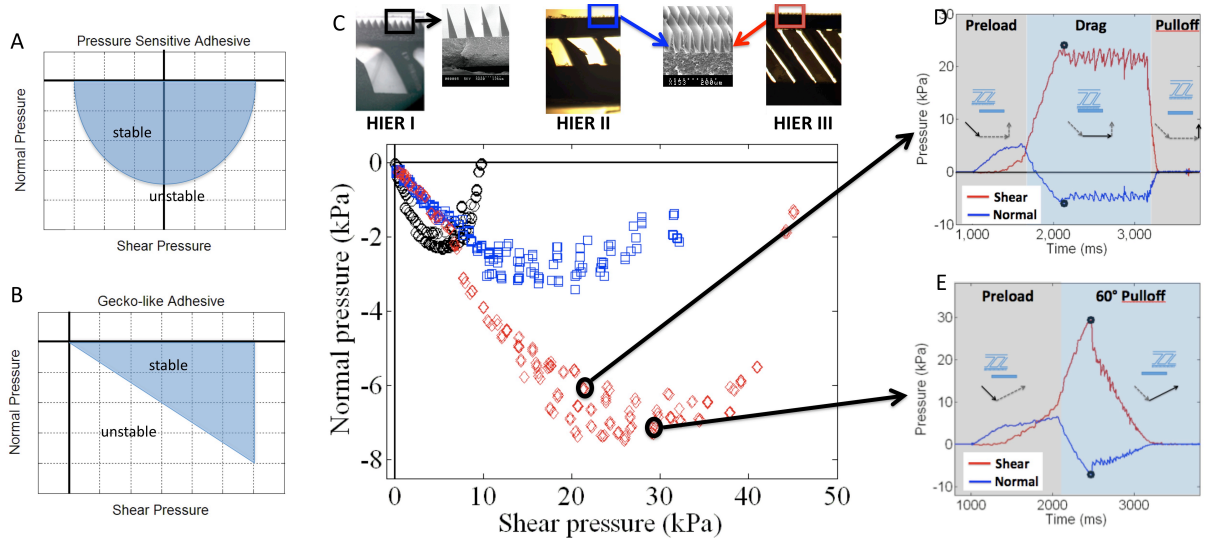

Figure 2: A) A typical pressure sensitive adhesive limit surface. Maximum adhesive force is obtained for pure normal pull-off and there is no zero-force detachment point. B) A frictional adhesive limit surface. Maximum adhesive force is only achieved when a shear loading is present in a preferred direction. Because the limit surface intersects the origin, a zero force detachment is possible when no shear loading is present. C) Empirically determined limit surfaces for the three hierarchical designs, Hierarchy I, II, and III. Each limit surface consists of many load-pull trials where a sample is loaded at a 45 degree angle in the preferred direction and then unloaded at an angle between 0 degrees (pure normal) and 90 degrees (drag). Insets show photos of these designs with magnified regions displaying contact features. D) Force-Time data for a single load-pull experiment with a 60 degree pulloff angle. Data points for the limit surface are circled. E) Force-time data for a single load-drag-pull experiment (90 degree pulloff) with the limit surface points circled.

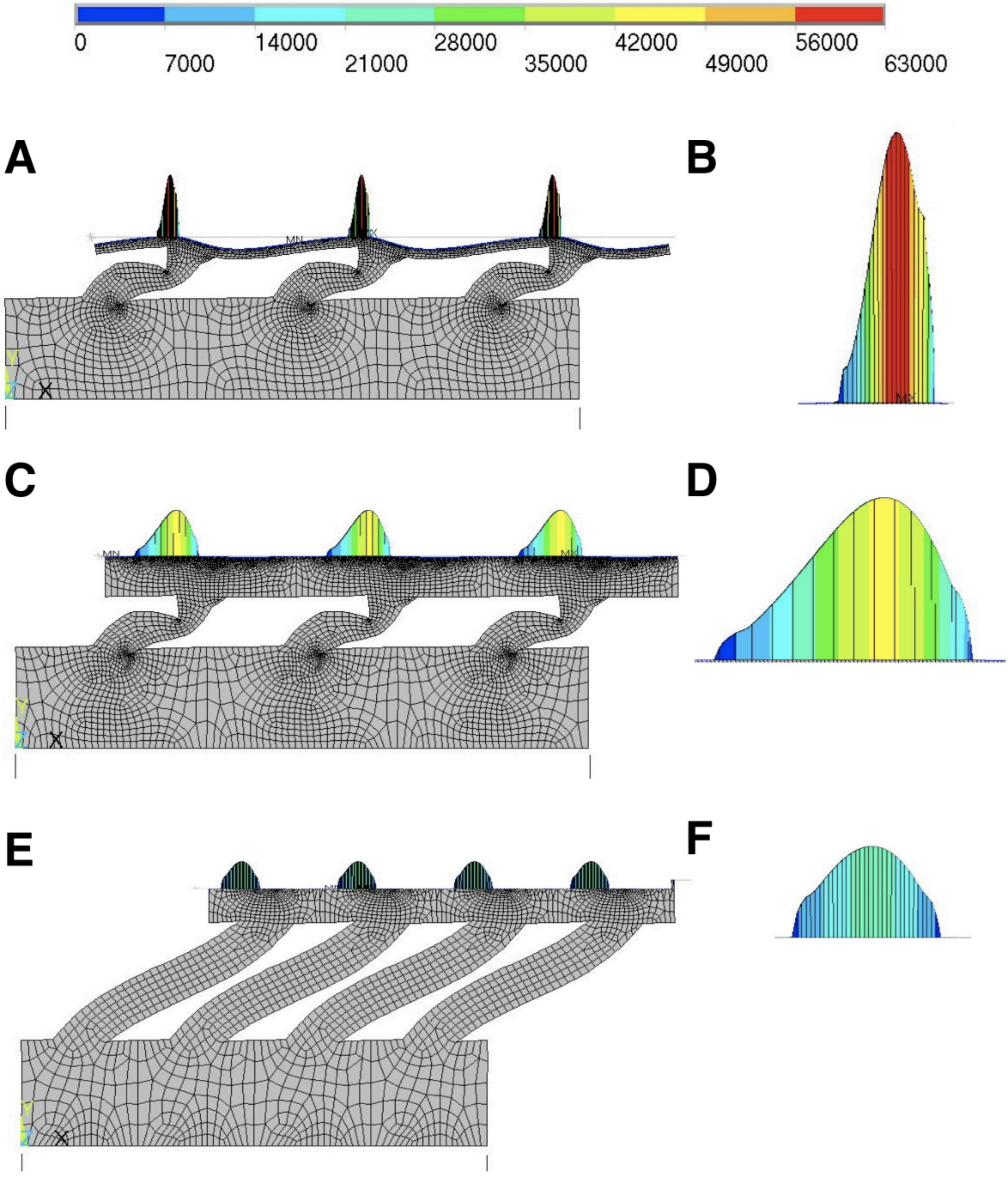

Figure 3: Finite element models to scale for A)Hierarchy I, C)Hierarchy II, and E)Hierarchy III. Each structure was simulated under a 45 degree preload to a depth of 500 μms. The pressure distributions for each model have been enlarged in B), D), and F). The scale bar represents Pascals of pressure.

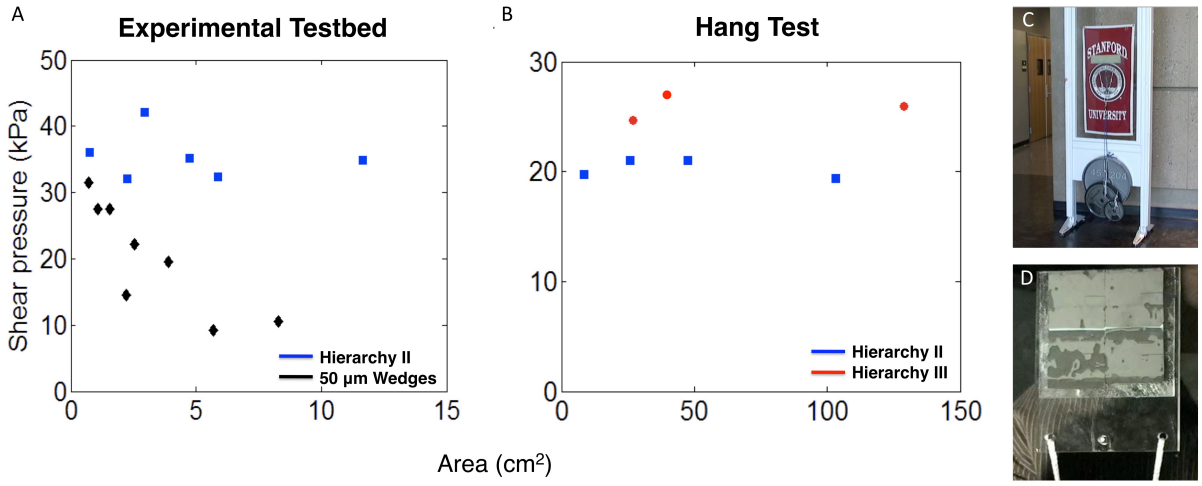

Figure 4: A) Data for identical experiments with various patch sizes for both the original 50 μm wedge shaped adhesive alone and the Hierarchy II design with 20 μm long wedges. Hierarchy II scales with patch size while the micro-structured wedge adhesive by itself suffers from alignment and load-sharing difficulties for patch sizes larger than 1 cm^2. B) Hanging weight experiments with both Hierarchy II and Hierarchy III on vertical glass showing the scalability of hierarchical designs out to greater than 100 cm^2. Hang tests typically yielded smaller pull-off pressures than measured on the experimental test platform, likely due to the change in loading scenario and rigidity of the system. C) The largest Hierarchy III patch fabricated held 35 kg on a vertical glass surface D) View through the reverse side of the vertical glass showing the true area of contact (light gray). For this 103 cm^2 patch, real area of contact is approximately 75 percent.

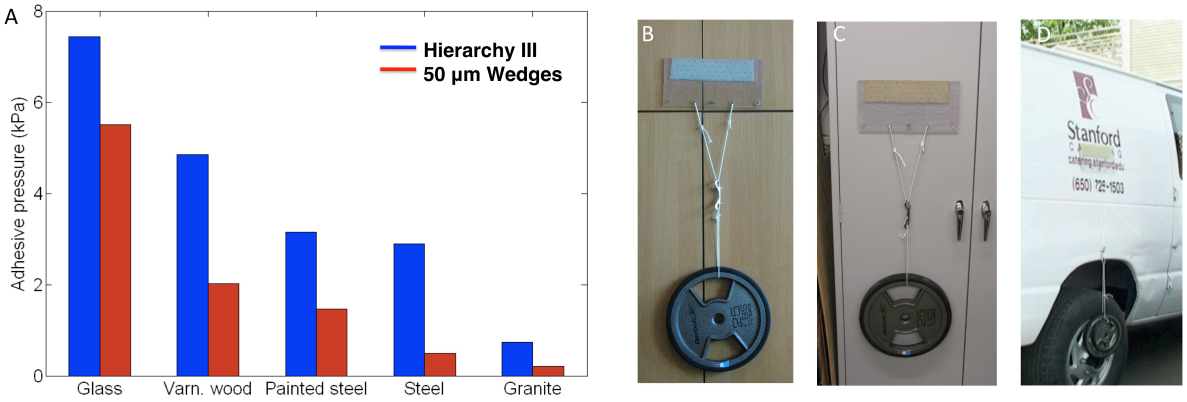

Figure 5: A) Hierarchy III samples performed well on a variety of semi-rough surfaces as well as glass. By comparison, the 50 μm wedge shaped adhesive by itself only performed well on very smooth surfaces. B) A large Hierarchy III patch demonstrating high levels of adhesion on a wood panel wall. The compliance of the suspension layer allows the sample to conform to a surface locally and compensate for large changes in roughness like the crack between adjacent panels. C) Hierarchy III patches also perform well on painted metal and D) real world uncleaned, unprepared surfaces like automobiles.

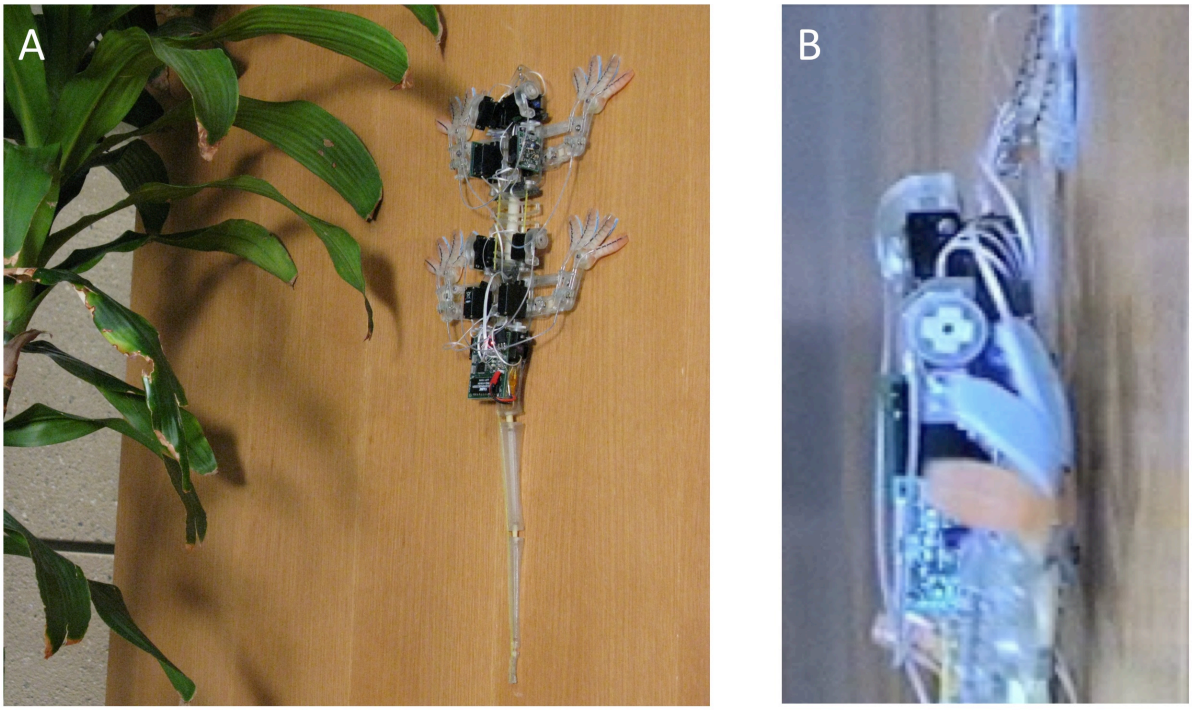

Figure 6: A) The Stickybot robot platform climbing with Hierarchy II adhesive toe pads. The robot was able to climb with a payload twice its bodyweight and climb both smooth surfaces like glass, and semi-rough surfaces like the wood panelling shown here and in B)